JACS
JOURNAL OF THE AMERICAN CHEMICAL SOCIETY
Communication
pubs.acs.org/JACS

Subnanometer Vacancy Defects Introduced on Graphene by Oxygen Gas

Yasuhiro Yamada,*[,†,⊥] Kazumasa Murota,[†,⊥] Ryo Fujita,[†] Jungpil Kim,[†] Ayuko Watanabe,[†] Masashi Nakamura,[†] Satoshi Sato,[†] Kenji Hata,[‡] Peter Ercius,[§] Jim Ciston,[§] Cheng Yu Song,[§] Kwanpyo Kim,[∥] William Regan,[∥] Will Gannett,[∥] and Alex Zettl[∥]

[†]Department of Applied Chemistry and Biotechnology, Chiba University, 1-33 Yayoi, Inage, Chiba 263-8522, Japan
[‡]National Institute of Advanced Industrial Science and Technology, Tsukuba, Ibaraki 305-8561, Japan
[§]National Center for Electron Microscopy, Lawrence Berkeley National Laboratory, Berkeley, California 94720, United States
[∥]Department of Physics, University of California at Berkeley, Berkeley, California 94720, United States

Supporting Information

ABSTRACT: The basal plane of graphene has been known to be less reactive than the edges, but some studies observed vacancies in the basal plane after reaction with oxygen gas. Observation of these vacancies has typically been limited to nanometer-scale resolution using microscopic techniques. This work demonstrates the introduction and observation of subnanometer vacancies in the basal plane of graphene by heat treatment in a flow of oxygen gas at low temperature such as 533 K or lower. High-resolution transmission electron microscopy was used to directly observe vacancy structures, which were compared with image simulations. These proposed structures contain C═O, pyran-like ether, and lactone-like groups.

Subnanometer vacancy defects in the basal plane of single-layer nanocarbon materials such as graphene and single-walled carbon nanotubes (SWCNTs) have been intensively studied because of a number of possible applications such as selective ion passage,[1] water desalination,[2] separation of gases,[3−5] impregnation of electrolytes,[6,7] and ligands to coordinate metal ions.[8,9] The most common methods to introduce vacancy defects on carbon materials are reactions with oxygen gas[4−7,10,11] and ion bombardment followed by oxidation.[10,12] Oxygen gas is superior to ion bombardment in terms of the accessibility of oxygen gas from multiple directions and the availability of oxygen gas. Thus, reactions of carbon materials with oxygen gas are still preferred for mass production.

Observations of graphite reacted with oxygen gas by optical microscopy have been reported since 1917.[13] Submicrometer hexagonal pits and holes have been observed in the basal plane of graphite after heat treatment in oxygen gas above 1073 K,[13,14] but the sizes of the pits are at the scale of optical microscopy. Recent studies have shown that pits with diameters of ca. 20 nm were formed in the basal plane of graphene heated in a flow of oxygen/argon gas at 723 K as determined by atomic force microscopy.[15] In related studies, subnanometer vacancy defects on carbon nanohorns were formed by heat treatment in oxygen gas above 573 K as determined by a molecular sieving method,[4,5] but defects observed by transmission electron microscopy (TEM) were larger than 1 nm.[6] These works have shown the existence and sizes of vacancy defects, whereas direct observations of the structures of vacancy defects including functional groups have not been obtained.

Functional groups at subnanometer defects introduced by ion bombardment followed by oxidation have been studied theoretically and experimentally. It has been reported that pyran-like ether, C═O, and lactone-like groups can be present at vacancy defects as shown by calculations,[16,17] and these functional groups were also confirmed by X-ray photoelectron spectroscopy (XPS).[18−20] However, the structures of subnanometer vacancy defects in the basal plane of graphene introduced simply by oxygen gas have not been directly observed.

We recently showed the relationship between the temperature and the density of vacancy defects on the walls of SWCNTs by the I_D/I_G intensity ratio using Raman spectroscopy,[7] where the D band (with intensity I_D) at ca. 1340 cm^{-1} originates from intervalley scattering and the G band (with intensity I_G) at 1580−1590 cm^{-1} originates from the Raman-active mode of graphite and SWCNTs.[21−23] The I_D/I_G ratio has been widely used to evaluate the disorder density in the basal plane of carbon materials.[7,15,24] The results suggest that the size of the vacancy defects becomes smaller as the oxidation temperature decreases. The onset temperature of the reaction of graphene with oxygen gas has been reported to range between 473 and 573 K as determined by the I_D/I_G ratio using Raman spectroscopy.[15] Thus, an oxidation temperature of graphene just above the onset temperature of the oxidation reaction is expected to be the threshold temperature to introduce subnanometer vacancy defects.

High-resolution TEM (HRTEM) is a powerful tool for direct imaging of defects in nanocarbon materials. With the progress of TEM aberration correction technology, subnanometer defects such as pentagons, heptagons, and point defects in the basal plane of graphene have been observed.[25−27] The defective structure of graphene oxide including oxygen-containing functional groups[28] and that of reduced graphene oxide including pentagons and heptagons[29] have been observed by HRTEM. However, the structures of the subnanometer vacancy defects

Received: November 26, 2013
Published: January 26, 2014

   dx.doi.org/10.1021/ja4117268 | J. Am. Chem. Soc. 2014, 136, 2232−2235

created in the basal plane of graphene by reaction with oxygen gas have not been directly observed by HRTEM.

In this work, the structures of subnanometer vacancy defects introduced in the basal plane of graphene by oxidation with O_2 were directly observed by HRTEM using the TEAM 0.5 microscope, and the stabilities of the structures were evaluated by density functional theory (DFT) calculation. In addition, high-surface-area graphite and large-diameter SWCNTs were oxidized and analyzed to support the defect structures of graphene observed using HRTEM.

Graphene was synthesized on both sides of a copper foil by chemical vapor deposition using methane and hydrogen gases at 1313 K.[30] The synthesized graphene was transferred to gold TEM grids without using a conventional polymer coating method[31] to avoid residues on the graphene [Figures S1 and S2 in the Supporting Information (SI)]. Graphene on the TEM grids was heated in vacuum at 773 K for 0.5 h (Figure S3) prior to oxidation at 493, 513, 533, 553, and 573 K for 5 and 24 h at an oxygen gas flow rate of 30 cm^3 min^{-1}. The oxidized graphene was further heated in vacuum at 773 K for 0.5 h to remove thermally unstable functional groups because the irradiation with electrons during observation may cause migration and decomposition of such functional groups.[28] HRTEM observations of graphene were carried out using the TEAM 0.5 aberration-corrected transmission electron microscope at 80 keV.[32] Optimizations of modeled structures and transition states were calculated by DFT using Gaussian 03.[33] Graphite and SWCNTs[34] were also oxidized in oxygen gas and analyzed by elemental analysis (Table S1 in the SI), Raman spectroscopy (JASCO NRS-2100, laser wavelength 532 nm), and XPS (Shimadzu AXIS ULTRA DLD) to support the results from the HRTEM images. Peaks in Raman spectra were fitted with Lorentzian-type line shapes based on the work done by Brown et al.[23]

Figure 1 shows HRTEM images of pristine graphene and defective graphene oxidized at 493, 513, and 533 K for 5 h. Fast Fourier transform mapping (Figure S3a)[35] and the I_{2D}/I_G intensity ratio (Figure S2a)[36] confirmed that the pristine graphene observed in Figure 1 was single-layer graphene. HRTEM images of graphene with the most vacancy defects at each temperature are shown in Figure 1. There was a tendency that vacancy defects were more easily found in the basal planes of graphene oxidized at higher temperatures. The density of subnanometer vacancy defects in graphene heated at 533 K was ca. 1 defect/100 nm^2 based on an average of 15 images. White spots in Figure 1a are adatoms, which desorbed during observation as indicated by Meyer et al.,[37] whereas white spots near the vacancy defects of oxidized graphene remained during observation (Figure 1b–d). Large defects observed in the basal plane of graphene tended to enlarge under electron irradiation (Figure 1c),[26] whereas a few small defects (Figure 1b,d) were stable during observation. Large-diameter SWCNTs heated in oxygen gas clearly showed that the I_D/I_G ratio increased as the temperature increased (Figure 2; see the SI for more detail), which supports the increase in defect density in the basal plane of graphene with temperature found in the HRTEM images.

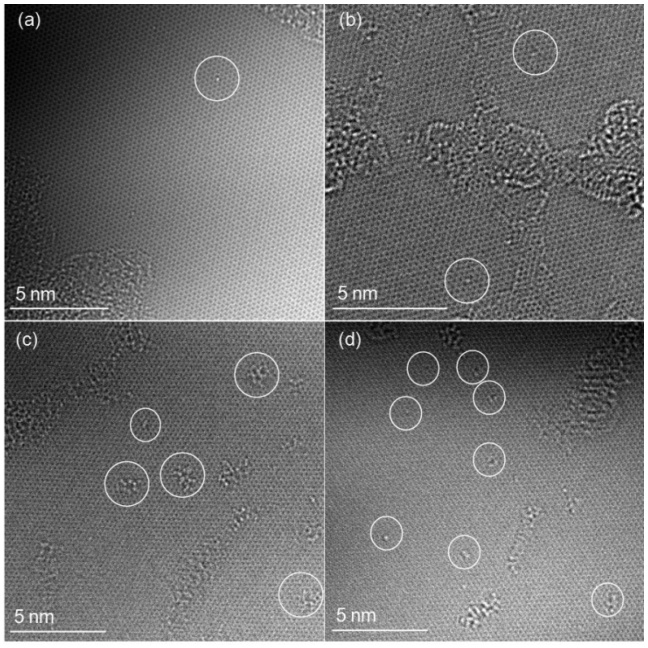

Figure 1. HRTEM images of (a) pristine graphene and (b–d) graphene oxidized for 5 h at (b) 493, (c) 513, and (d) 533 K. An adatom in (a) and defects in (b–d) are marked by white circles. All images were observed using different graphene samples.

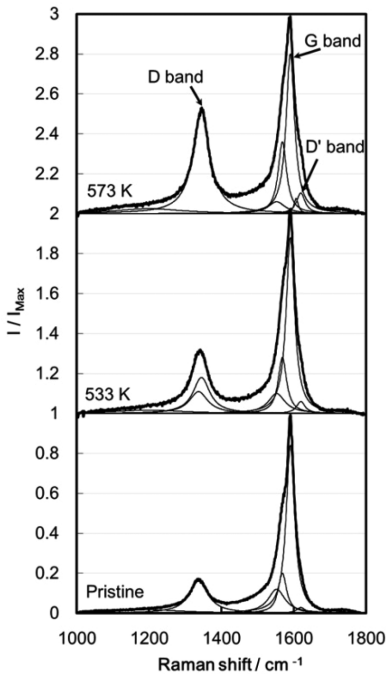

Figure 2. Raman spectra of pristine SWCNTs and SWCNTs heated in oxygen gas at 533 and 573 K for 168 h.

Graphite heated in oxygen gas at 493, 533, and 573 K for 5 and 24 h showed increasing oxygen content as the temperature increased (Table S1 and Figure 3). The increment of peak 1 in the O 1s XPS spectra (corresponding to C═O and C═O in lactone) and peak 3 (corresponding to pyran-like ether and C–O–C in lactone)[18,20,38] were increased above 533 K. These functional groups are indications of vacancy defects in the basal plane of graphite (see the SI for more detail). Thus, it is proved that the vacancy defects introduced in the basal plane of graphene (Figure 1b–d) were introduced by oxygen gas upon heating.

The HRTEM images of stable defects in the basal plane of graphene heated at 533 K for 5 h were further analyzed by focal series reconstruction (Figure 4a1,b1). The corresponding estimated structures and their simulated HRTEM phase images are shown in Figure 4a2,b2 and Figure 4a4,b4, respectively.

dx.doi.org/10.1021/ja4117268 | J. Am. Chem. Soc. 2014, 136, 2232–2235

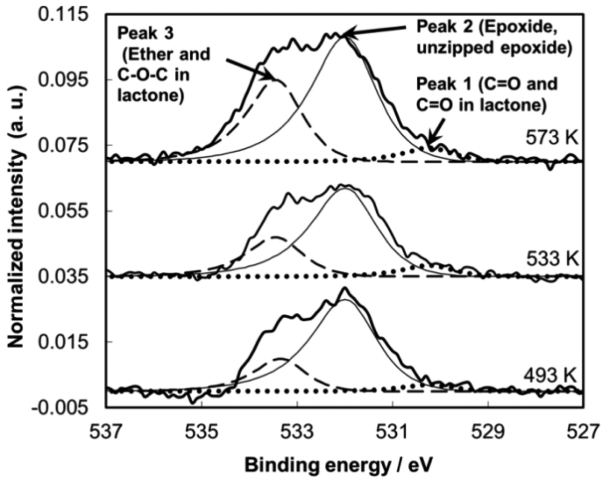

Figure 3. O 1s XPS difference spectra of graphite heated in oxygen gas for 5 h at different temperatures. The O 1s spectrum of graphite was subtracted from each spectrum. Bold lines: original spectra. Dotted lines: peak 1. Thin lines: peak 2. Dashed lines: peak 3.

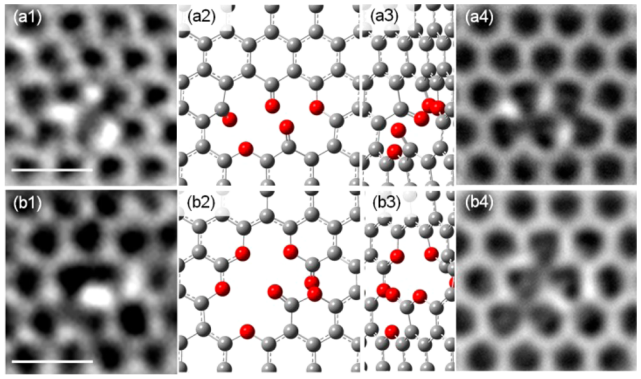

Figure 4. Phase images calculated by HRTEM exit-wave reconstruction, proposed atomic structures, and corresponding simulated HRTEM images of graphene heated at 533 K for 5 h. (a1, b1) Reconstructed HRTEM phase images. (a2, b2) Estimated structures of (a1) and (b1), with C atoms in gray and O-containing functional groups in red. (a3, b3) Perspective views of (a2) and (b2). (a4, b4) Simulated HRTEM phase images of (a2) and (b2). Scale bars are 0.5 nm.

These estimated structures were constructed on the basis of the difference of in- and out-of-plane oxygen (Figure S4) and of the reported calculated results that gasification of oxygen-containing functional groups does not form dangling bonds to minimize the energy.[17,39] Figure 4a3,b3 shows that oxygen-containing functional groups such as C═O are out of the basal plane of graphene. Indeed, atoms in simulated images of these functional groups (Figure 4a4,b4 and Figure S5a4,b4) are higher in brightness than other atoms. Out-of-plane oxygen-containing functional groups such as hydroxyl groups and epoxide in the basal plane of graphene oxide have been observed,[28] whereas in-plane oxygen-containing functional groups are reported to be difficult to differentiate from other atoms such as carbon atoms.[40]

Functional groups such as C═O, pyran-like ether, and lactone-like groups on edges have been reported as stable functional groups,[16,17,38] whereas epoxides and OH groups in the basal plane of graphene are known as relatively unstable functional groups.[17,19,38] For example, the migrations of oxygen-containing functional groups such as epoxide and hydroxyl groups in graphene oxide require 2.1 and 0.7 eV, respectively.[28,41] Another research group reported that the migration of epoxide in the basal plane of graphene requires 1.0–1.5 eV.[42] These energies are much lower than the C–C bond energy of graphene (4.9 eV) and are easily disturbed by the incoming 80 keV electron beam.[43]

The stabilities of our proposed structures containing stable functional groups in Figure 4a2,b2 were determined by calculating activation energies. The activation energy required for migration of one oxygen atom from C═O at the 4,5-position of a phenanthrene-like structure (Figures 4a2 and S6b1) was the lowest (2.5 eV) among all functional groups in Figure 4a2. The activation energy required for migration of one oxygen atom from a lactone-like structure (Figures 4b2 and S7b1) was the lowest (2.3 eV) among functional groups in Figure 4b2. These activation energies are higher than those for the migration of epoxide and hydroxyl groups observed previously by HRTEM.[28] In addition, the similarities of the simulated HRTEM images in Figure 4a4,b4 to the actual HRTEM images in Figure 4a1,b1 were high. Thus, the structures in Figure 4a2,b2 were selected as the proposed structures. We investigated other possible structures (Figure S5a2,b2), but these structures were neither stable (Figures S8 and S9) nor the same appearance (Figure S5a4,b4) compared with the actual HRTEM images in Figure 4a1,b1. Thus, the presence of C═O, pyran-like ether, and lactone-like groups in Figure 4 can be explained from the viewpoints of HRTEM images as well as their stabilities.

In conclusion, HRTEM images of subnanometer vacancy defects in graphene oxidized for 5 h at 533 K or lower could be obtained. Since subnanometer vacancy defects were observed at 533 K, the onset temperature of the oxidation reaction of the basal plane of graphene must be lower than 533 K. Experimental exit-phase images matched the simulated images of the proposed structures at the atomic scale. The proposed structures contain C═O, pyran-like ether, and lactone-like functional groups. The presence of the proposed structures could also be explained by the stability of the structures. Oxygen-containing functional groups such as C═O and C–O–C detected by XPS spectra of graphite and the increment of the I_D/I_G ratio of SWCNTs are also evidence of the presence of vacancy defects in the basal plane of a single-layer graphene.

■ ASSOCIATED CONTENT

Ⓢ Supporting Information

Experimental methods and additional results. This material is available free of charge via the Internet at http://pubs.acs.org.

■ AUTHOR INFORMATION

Corresponding Author

y-yamada@faculty.chiba-u.jp

Author Contributions

⊥Y.Y. and K.M. contributed equally.

Notes

The authors declare no competing financial interest.

■ ACKNOWLEDGMENTS

Acknowledgments are made to the Kagoshima University in Japan for XPS measurements. Graphite was supplied from Nippon Graphite Industries, Ltd. This work was supported by the Japan Society for the Promotion of Science (JSPS) KAKENHI Grant 22760594, the JSPS Institutional Program for Young Researcher Overseas Visits, the Murata Science Foundation for an overseas visit, and the Yazaki Memorial

Foundation for Science and Technology for an overseas visit. A portion of this work was performed at NCEM, which is supported by the U.S. Department of Energy, Office of Science, Office of Basic Energy Sciences under Contract DE-AC02-05CH11231.

REFERENCES

(1) Sint, K.; Wang, B.; Král, P. *J. Am. Chem. Soc.* **2008**, *130*, 16448.
(2) Cohen-Tanugi, D.; Grossman, J. C. *Nano Lett.* **2012**, *12*, 3602.
(3) Du, H.; Li, J.; Zhang, J.; Su, G.; Li, X.; Zhao, Y. *J. Phys. Chem. C* **2011**, *115*, 23261.
(4) Ohba, T.; Kanoh, H.; Kaneko, K. *Chem. Lett.* **2011**, *40*, 1089.
(5) Murata, K.; Hirahara, K.; Yudasaka, M.; Iijima, S.; Kasuya, D.; Kaneko, K. *J. Phys. Chem. B* **2002**, *106*, 12668.
(6) Yang, C. M.; Kim, Y. J.; Endo, M.; Kanoh, H.; Yudasaka, M.; Iijima, S.; Kaneko, K. *J. Am. Chem. Soc.* **2007**, *129*, 20.
(7) Yamada, Y.; Kimizuka, O.; Machida, K.; Suematsu, S.; Tamamitsu, K.; Saeki, S.; Yamada, Y.; Yoshizawa, N.; Tanaike, O.; Yamashita, J.; Don, F.; Hata, K.; Hatori, H. *Energy Fuels* **2010**, *24*, 3373.
(8) Stoyanov, S. R.; Titov, A. V.; Král, P. *Coord. Chem. Rev.* **2009**, *253*, 2852.
(9) Yamada, Y.; Miyauchi, M.; Kim, J.; Takai, K. H.; Sato, Y.; Suenaga, K.; Ohba, T.; Sodesawa, T.; Sato, S. *Carbon* **2011**, *49*, 3375.
(10) Hahn, J. R. *Carbon* **2005**, *43*, 1506.
(11) Stevens, F.; Kolodny, L. A.; Beebe, T. P., Jr. *J. Phys. Chem. B* **1998**, *102*, 10799.
(12) Kholmanov, I. N.; Edgeworth, J.; Cavaliere, E.; Gavioli, L.; Magnuson, C.; Ruoff, R. S. *Adv. Mater.* **2011**, *23*, 1675.
(13) Thomas, J. M. *Chem. Phys. Carbon* **1965**, *1*, 122.
(14) Geer, E. N.; Topley, B. *Nature* **1932**, *129*, 904.
(15) Liu, L.; Ryu, S.; Tomasik, M. R.; Stolyarova, E.; Jung, N.; Hybertsen, M. S.; Steigerwald, M. L.; Brus, L. E.; Flynn, G. W. *Nano Lett.* **2008**, *8*, 1965.
(16) Carlsson, J. M.; Hanke, F.; Linic, S.; Scheffler, M. *Phys. Rev. Lett.* **2009**, *102*, 166104.
(17) Sun, T.; Fabris, S.; Baroni, S. *J. Phys. Chem. C* **2011**, *115*, 4730.
(18) Larciprete, R.; Lacovig, P.; Gardonio, S.; Baraldi, A.; Lizzit, S. *J. Phys. Chem. C* **2012**, *116*, 9900.
(19) Larciprete, R.; Fabris, S.; Sun, T.; Lacovig, P.; Baraldi, A.; Lizzit, S. *J. Am. Chem. Soc.* **2011**, *133*, 17315.
(20) Barinov, A.; Malcioglu, O. B.; Fabris, S.; Sun, T.; Gregoratti, L.; Dalmiglio, M.; Kiskinova, M. *J. Phys. Chem. C* **2009**, *113*, 9009.
(21) Jorio, A.; Saito, R.; Dresselhaus, G.; Dresselhaus, M. S. *Philos. Trans. R. Soc., A* **2004**, *362*, 2311.
(22) Dresselhaus, M. S.; Dresselhaus, G.; Saito, R.; Jorio, A. *Phys. Rep.* **2005**, *409*, 47.
(23) Brown, S. D. M.; Jorio, A.; Corio, P.; Dresselhaus, M. S.; Dresselhaus, G.; Saito, R.; Kneipp, K. *Phys. Rev. B* **2001**, *63*, No. 155414.
(24) Eckmann, A.; Felten, A.; Mishchenko, A.; Britnell, L.; Krupke, R.; Novoselov, K. S.; Casiraghi, C. *Nano Lett.* **2012**, *12*, 3925.
(25) Hashimoto, A.; Suenaga, K.; Gloter, A.; Urita, K.; Iijima, S. *Nature* **2004**, *430*, 870.
(26) Girit, C. O.; Meyer, J. C.; Erni, R.; Rossell, M. D.; Kisielowski, C.; Yang, L.; Park, C. H.; Crommie, M. F.; Cohen, M. L.; Louie, S. G.; Zettl, A. *Science* **2009**, *323*, 1705.
(27) Banhart, F.; Kotakoski, J.; Krasheninnikov, A. V. *ACS Nano* **2011**, *5*, 26.
(28) Erickson, K.; Erni, R.; Lee, Z.; Alem, N.; Gannett, W.; Zettl, A. *Adv. Mater.* **2010**, *22*, 4467.
(29) Gómez-Navarro, C.; Meyer, J. C.; Sundaram, R. S.; Chuvilin, A.; Kurasch, S.; Burghard, M.; Kern, K.; Kaiser, U. *Nano Lett.* **2010**, *10*, 1144.
(30) Li, X.; Cai, W.; An, J.; Kim, S.; Nah, J.; Yang, D.; Piner, R.; Velamakanni, A.; Jung, I.; Tutuc, E.; Banerjee, S. K.; Colombo, L.; Ruoff, R. S. *Science* **2009**, *324*, 1312.
(31) Li, X.; Zhu, Y.; Cai, W.; Borysiak, M.; Han, B.; Chen, D.; Piner, R. D.; Colombo, L.; Ruoff, R. S. *Nano Lett.* **2009**, *9*, 4359.
(32) Daiimen, U.; Erni, R.; Radmilovic, V.; Kisielowski, C.; Rossell, M. D.; Denes, P. *Philos. Trans. R. Soc., A* **2009**, *367*, 3795.
(33) Frisch, M. J.; Trucks, G. W.; Schlegel, H. B.; Scuseria, G. E.; Robb, M. A.; Cheeseman, J. R.; Montgomery, J. A., Jr.; Vreven, T.; Kudin, K. N.; Burant, J. C.; Millam, J. M.; Iyengar, S. S.; Tomasi, J.; Barone, V.; Mennucci, B.; Cossi, M.; Scalmani, G.; Rega, N.; Petersson, G. A.; Nakatsuji, H.; Hada, M.; Ehara, M.; Toyota, K.; Fukuda, R.; Hasegawa, J.; Ishida, M.; Nakajima, T.; Honda, Y.; Kitao, O.; Nakai, H.; Klene, M.; Li, X.; Knox, J. E.; Hratchian, H. P.; Cross, J. B.; Bakken, V.; Adamo, C.; Jaramillo, J.; Gomperts, R.; Stratmann, R. E.; Yazyev, O.; Austin, A. J.; Cammi, R.; Pomelli, C.; Ochterski, J. W.; Ayala, P. Y.; Morokuma, K.; Voth, G. A.; Salvador, P.; Dannenberg, J. J.; Zakrzewski, V. G.; Dapprich, S.; Daniels, A. D.; Strain, M. C.; Farkas, O.; Malick, D. K.; Rabuck, A. D.; Raghavachari, K.; Foresman, J. B.; Ortiz, J. V.; Cui, Q.; Baboul, A. G.; Clifford, S.; Cioslowski, J.; Stefanov, B. B.; Liu, G.; Liashenko, A.; Piskorz, P.; Komaromi, I.; Martin, R. L.; Fox, D. J.; Keith, T.; Al-Laham, M. A.; Peng, C. Y.; Nanayakkara, A.; Challacombe, M.; Gill, P. M. W.; Johnson, B.; Chen, W.; Wong, M. W.; Gonzalez, C.; Pople, J. A. *Gaussian 03*, revision C.02; Gaussian, Inc.: Wallingford CT, 2004.
(34) Hata, K.; Futaba, D. N.; Mizuno, K.; Namai, T.; Yumura, M.; Iijima, S. *Science* **2004**, *306*, 1362.
(35) Kim, K.; Lee, Z.; Regan, W.; Kisielowski, C.; Crommie, M. F.; Zettl, A. *ACS Nano* **2011**, *5*, 2142.
(36) Ferrari, A. C.; Meyer, J. C.; Scardaci, V.; Casiraghi, C.; Lazzeri, M.; Mauri, F.; Piscanec, S.; Jiang, D.; Novoselov, K. S.; Roth, S.; Geim, A. K. *Phys. Rev. Lett.* **2006**, *97*, No. 187401.
(37) Meyer, J. C.; Girit, C. O.; Crommie, M. F.; Zettl, A. *Nature* **2008**, *454*, 319.
(38) Yamada, Y.; Yasuda, H.; Murota, K.; Nakamura, M.; Sodesawa, T.; Sato, S. *J. Mater. Sci.* **2013**, *48*, 8171.
(39) Ma, Y.; Lehtinen, P. O.; Foster, A. S.; Niemine, R. M. *New J. Phys.* **2004**, *6*, 68.
(40) Kurasch, S.; Meyer, J. C.; Kunzel, D.; Groß, A.; Kaiser, U. *Beilstein J. Nanotechnol.* **2011**, *2*, 394.
(41) Lahaye, R. J. W. E.; Jeong, H. K.; Park, C. Y.; Lee, Y. H. *Phys. Rev. B* **2009**, *79*, No. 125435.
(42) Radovic, L. R.; Suarez, A.; Vallejos-Burgos, F.; Sofo, J. O. *Carbon* **2011**, *49*, 4226.
(43) Brenner, D. W.; Shenderova, O. A.; Harrison, J. A.; Stuart, S. J.; Ni, B.; Sinnott, S. B. *J. Phys.: Condens. Matter* **2002**, *4*, 783.